

## ECOLOGY

## The rise of compound warm-season droughts in Europe

Yannis Markonis<sup>1\*</sup>, Rohini Kumar<sup>2</sup>, Martin Hanel<sup>1,3,4</sup>, Oldrich Rakovec<sup>1,2</sup>, Petr Máca<sup>1</sup>, Amir AghaKouchak<sup>5</sup>

Drought is one of the main threats to food security and ecosystem productivity. During the past decades, Europe has experienced a series of droughts that caused substantial socioeconomic losses and environmental impacts. A key question is whether there are some similar characteristics in these droughts, especially when compared to the droughts that occurred further in the past. Answering this question is impossible with traditional single-index approaches and also short-term and often spatially inconsistent records. Here, using a multidimensional machine learning–based clustering algorithm and the hydrologic reconstruction of European drought, we determine the dominant drought types and investigate the changes in drought typology. We report a substantial increase in shorter warm-season droughts that are concurrent with an increase in potential evapotranspiration. If shifts reported here persist, then we will need new adaptive water management policies and, in the long run, we may observe considerable alterations in vegetation regimes and ecosystem functioning.

## INTRODUCTION

Since the beginning of the 21st century, Europe has been repeatedly hit by severe drought events with serious socioeconomic consequences (1). Concern has been raised about whether there is an increase in drought frequency, duration, or intensity (2, 3) and most importantly, to what extent the observed global warming has altered the European droughts (4, 5). There is a general agreement that, during the past decades, less droughts have occurred in Northern Europe (NEU), while a drying pattern has been observed in the Mediterranean (MED) region and mixed (and even opposing) patterns in Central (CEU) and Eastern Europe (2, 5–8). In most of the previous studies, one single drought index is used to detect and quantify changes in droughts. However, there are more than 70 operational/research indices (9, 10), most of which only reveal one particular aspect of a drought (e.g., deficit in precipitation) and cannot be used as comprehensive indicators (11). This is because drought is a complex phenomenon. Its evolution involves a large number of processes across the atmosphere, hydrosphere, lithosphere, and biosphere. Thus, it is extremely challenging, if not impossible, to create a single index that fully depicts drought in an objective and holistic way. Plausible alternatives are either quantifying the underlying energy and mass fluxes through hydrological modeling (12) or applying a drought typology that corresponds to specific physical mechanisms including drought onset, propagation, and termination (13). If we combine these two, instead of analyzing one or more drought indices, then we can study changes in drought types in a process-based approach. Up to this day, drought typology has been applied only to characterize hydrological drought in parts of European territories, such as Finland (14), Germany (15), and Alps (16). However, no study exists that investigates how drought types have changed in either regional or continental regimes.

<sup>1</sup>Faculty of Environmental Sciences, Czech University of Life Sciences Prague, Praha-Suchbát 16500, Czech Republic. <sup>2</sup>UFZ-Helmholtz Centre for Environmental Research, Leipzig 04318, Germany. <sup>3</sup>Department of Hydrology, T. G. Masaryk Water Research Institute, Podbabská 2582/30, Prague 6 160 00, Czech Republic. <sup>4</sup>Global Change Research Institute, CAS, Bělidla 986/4b, Brno 603 00, Czech Republic. <sup>5</sup>Department of Civil and Environmental Engineering and Department of Earth System Science, University of California, Irvine, Irvine, CA 92697, USA.

\*Corresponding author. Email: markonis@fzp.czu.cz

Here, we use drought typology to assess the fluctuations of European drought seasonality and duration since 1900. To achieve this, we use temperature and precipitation time series from observational data and simulate runoff and soil moisture with the mesoscale hydrological model (mHM) (17, 18). The model was set up and validated at a 50 × 50-km spatial scale and daily resolution in a previous study (19). The validation showed that data uncertainties and different potential evapotranspiration (PET) estimators do not significantly influence the simulation results since 1900 (19, 20). To explore changes in the regional characteristics, we divided the European domain into three regions (fig. S1), namely, NEU, CEU, and MED. Then, for each grid cell, we estimated the deficit volumes of 3-month mean precipitation, monthly runoff, and monthly soil moisture to describe meteorological, hydrological, and agricultural droughts, respectively. Instead of using an a priori definition of specific drought types, we applied an unsupervised machine learning classification algorithm based on self-organizing maps (SOMs) (21) to determine the events sharing similar temporal features. We consider 5 × 5 SOM to classify different drought events with at least 3 months of duration. The resulting 25 SOM nodes were summarized through hierarchical agglomerative clustering to determine the dominant characteristic classes (see Materials and Methods).

## RESULTS

The classification reveals three major classes of European drought events (Fig. 1, classes A to C) that peak in summer (A), autumn (B), and winter (C), respectively. Although their seasonality is common across all three regions, the underlying processes that drive them are not the same. In CEU and NEU, summer droughts are initiated in spring or early summer because of lack of rainfall and high evapotranspiration and last for 4 months on average. We shall call these events “compound warm-season droughts” because of the compounding impacts of low precipitation and high temperatures. It has been found that these droughts are connected or exacerbated by concurrent heat waves (22–25). In MED, summer droughts are initiated by precipitation deficits during the cold and wet period (late winter to early spring), and thus, their mean duration is longer, reaching 7 months. These droughts have been already identified as wet-to-dry season droughts (26). Autumn droughts are similar in

Copyright © 2021  
The Authors, some  
rights reserved;  
exclusive licensee  
American Association  
for the Advancement  
of Science. No claim to  
original U.S. Government  
Works. Distributed  
under a Creative  
Commons Attribution  
NonCommercial  
License 4.0 (CC BY-NC).

Downloaded from https://www.science.org on September 03, 2021

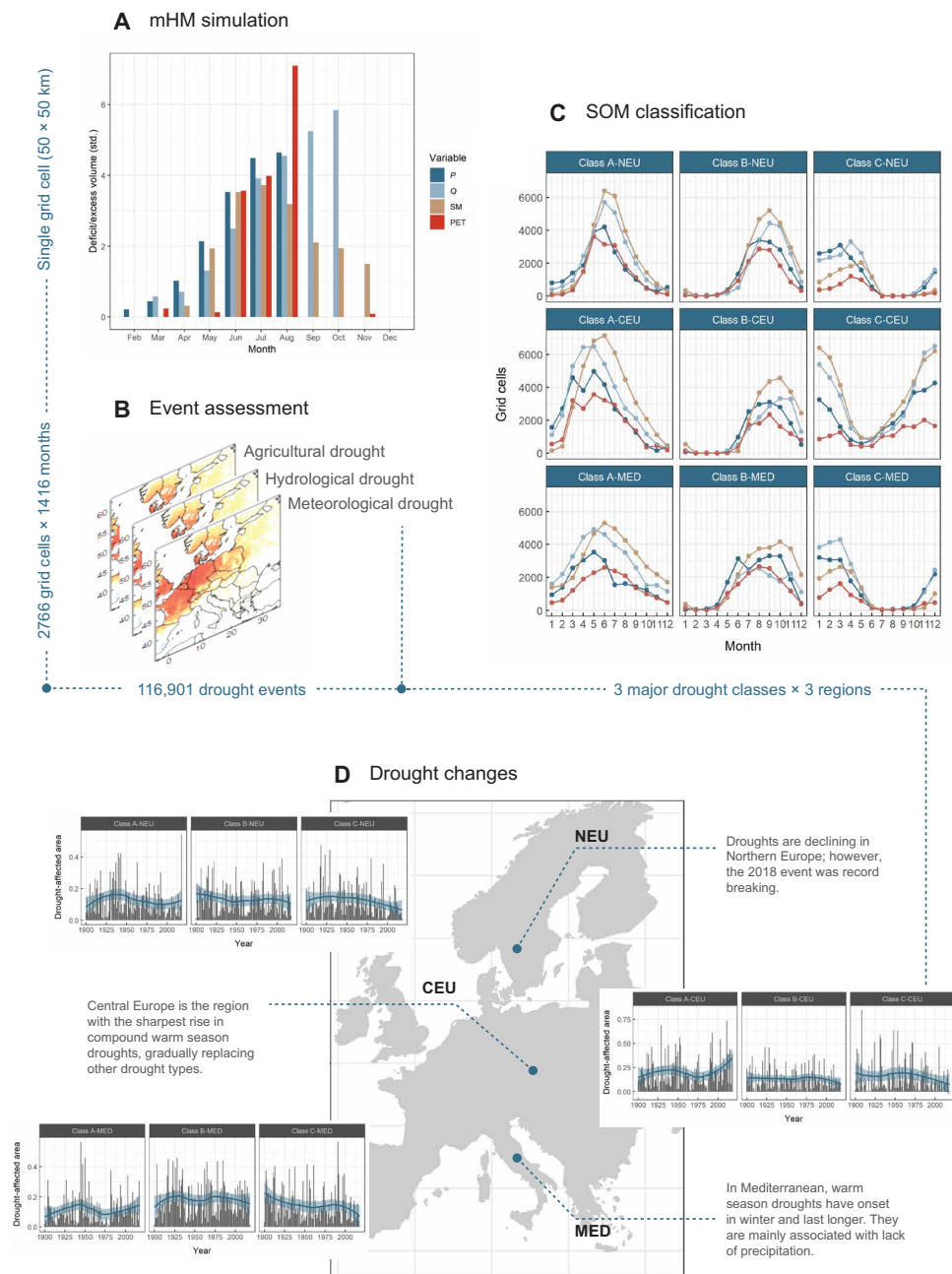


**Fig. 1. Classification of drought events.** (A) The mHM simulation produces time series of runoff and soil moisture using precipitation and temperature at each grid cell (50 × 50 km). (B) Three types of drought (meteorological, hydrological, and agricultural) are determined, and the events that last for at least 3 months are assessed for each grid cell. (C) The machine learning classification scheme reduces the dimensionality of the issue to three major drought classes for NEU, CEU, and MED. The borders of the three regions are presented in fig. S1. Each pointed line represents the number of grid cells under drought due to deficit in precipitation (P), runoff (Q), and soil moisture (SM) or excess PET [colors are as in (A)]. (D) The temporal evolution of annual drought coverage per class and region highlights current drought dynamics (loess regression).

all regions and are the classical rainfall deficit droughts—the most common type of droughts in this region (13). In winter, we observe rain-to-snow season droughts in CEU and NEU (13). They are initiated by rainfall deficit in the late rainy season (summer and autumn) and propagate to the snow season (winter). In MED, winter droughts can be either rain-to-snow season or classical rainfall deficit droughts, as a consequence of the climatic heterogeneity and variability of the MED region. These are the main processes related by the drought types identified by the classification scheme.

Regardless of their physical causes, the number of warm-season droughts is increasing in the largest part of Europe (Fig. 1D). The most abrupt shift is observed in CEU (above 0.99 quantile; fig. S2), where one-third of the most extensive compound warm-season events occurred in the past 15 years. After the well-known drought of 2003, similar events also happened in 2007, 2011, 2012, 2015, and 2018. The last one also affected NEU at an unprecedented extent (fig. S2). At the same time, the rain-to-snow season droughts are in decline. Barnett *et al.* (27) suggested that the transition from

rain-to-snow season droughts to warm-season droughts would happen in snow-dominated regions because of earlier snowmelt. The latter has already been reported for Europe (28). In addition, the observed increase in liquid precipitation during winter (29) might decrease drought in the cold season, but it also favors conditions for the development of agricultural droughts in the summer because snow cover is linked with soil water storage (30).

In MED, there is an increase in wet-to-dry season droughts (in the top 0.1 quantile; fig. S2), associated with the decline of winter precipitation (31, 32). This confirms the prevailing hypothesis that the drying is mainly associated with a change in winter precipitation (2), although the strength of the decline in the precipitation has been questioned (33). It is noteworthy that low winter precipitation in MED also affects Central European summer droughts as noted by Vautard *et al.* (34). They argued that low soil moisture dries air masses in Southern Europe, which, as they move northward, decrease cloudiness and enhance the atmospheric evaporative demand. Our hydrologic simulation is in agreement with their hypothesis, showing that, during the compound warm-season events of CEU, January to April soil moisture deficits in MED were 20% higher than the rest

years. Therefore, the increase in MED wet-to-dry season droughts could possibly be linked to the increase of Central European compound warm-season events. We have to note, though, that the increase in MED precedes the increase in CEU for a decade (fig. S2).

NEU does not follow the warm-season drought trend discussed earlier. Mostly in Scandinavia, droughts are becoming markedly less frequent, both in absolute number (less than 0.1 quantile or even less than 0.01 quantile if the 2018 drought is not considered; fig. S2) and during summer. This is consistent with the expectation and strong evidence that high latitudes are getting wetter (fig. S3) (35), exceeding the millennial climatic maximum (36). Nevertheless, warm-season droughts in NEU are also subject to a significant shift. We have investigated how the climatic variables (temperature and precipitation) are related to drought to unravel their potential effect in drought (Fig. 2). In the beginning of the 20th century, the duration of precipitation deficit was, on average, three times higher than excessive PET (Fig. 2A). On the contrary, during the past 2 decades, excessive PET slightly outlasted precipitation, following an almost monotonic increase in all regions. In addition, as global air temperature increased, drought initiation has been more often

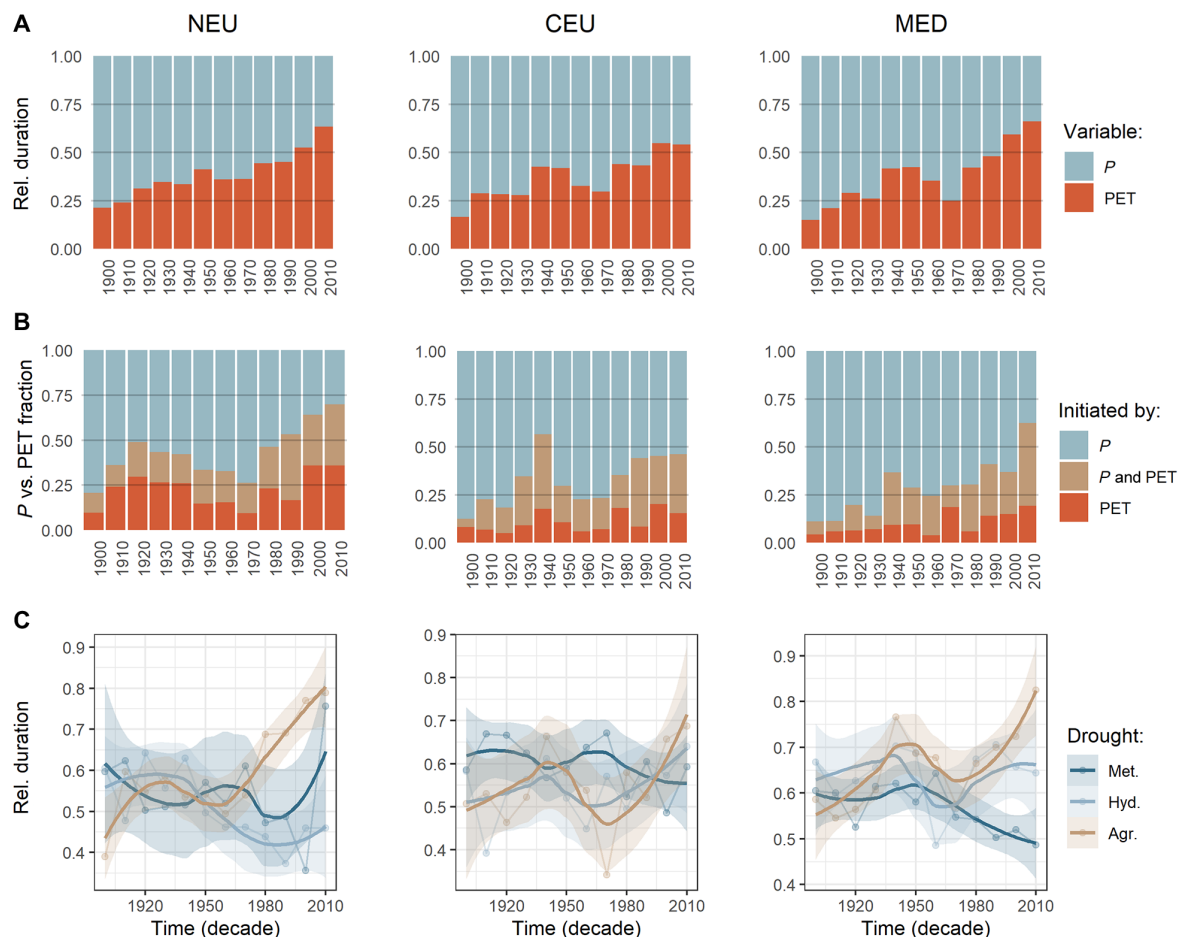


**Fig. 2. Decadal changes in onset and propagation of compound warm season events.** (A) Ratio of average duration of deficit  $P$  versus excessive PET during drought events. (B) Hydroclimatic variables associated to drought onset, described as the fraction of drought events per decade initiated by precipitation ( $P$ ), PET, and both ( $P$  and PET). Initiation is determined when there is precipitation deficit or excessive PET in the month that the drought event started. (C) Relative duration of each drought type. The relative duration is estimated by dividing the duration under meteorological, hydrological, and agricultural droughts by the total duration of each event. The mean of the duration fraction is presented per year and type of drought.

associated with excessive PET (Fig. 2B). The most pronounced change is observed in NEU, where drought events starting in months with solely precipitation deficits have fallen from 80% to less than 20%. In MED, the change is more monotonic and the drop was from 90% to less than 50%, while, in CEU, the shift is more subtle. Therefore, it is highly likely that evapotranspiration has become more involved as a driving factor in drought onset.

## DISCUSSION

The effect of increased PET is mostly evident in the soil moisture deficits and the associated agricultural droughts. We see that, during each summer drought event, the number of months with soil moisture deficit has been increasing in all regions (Fig. 2C). In the past decades, when there is a compound warm-season event, during most time agricultural drought is present. That ranges between approximately 75 and 85% of the total event duration on average and is the centennial maximum. What is alarming is that the duration of meteorological droughts is declining, implying that the high atmospheric evaporative demand, already confirmed in various locations across Europe (3, 37–40), is extending the total event duration. Agricultural and hydrological droughts present quite similar patterns in their fluctuations for CEU and MED. This is less evident in NEU, but this region is distinctly more affected by the snow dynamics. This could mean that there are no or low deficits in the water reservoirs/groundwater, especially since we observe an increase in precipitation (fig. S3). On the contrary, in the warm-season drought events, we observe a rapid increase of excessive PET, which can result to excessive evapotranspiration that will deplete soil moisture and cause agricultural drought. In this case, the impact to the water reservoirs/groundwater is less profound because of the role of the preceding conditions (41). All these factors indicate a persistent amplification of agricultural droughts that could be associated to global warming (42).

This increasing type of droughts is also evident in climate model projections (43–47). However, this does not necessarily imply a causal relationship between the increase in atmospheric evaporative demand and the rise of warm-season droughts. This is because the drivers of atmospheric evaporative demand present high complexity (48), which cannot be fully captured in PET-driven hydrological simulations. For example, reduced cloudiness due to changes in atmospheric circulation could be the main driver for the warm-season drought events (49). Another challenge lies in quantifying the vegetation transpiration response to elevated CO<sub>2</sub>. The water use efficiency of plants has a direct impact in PET, but its overall effect in drought remains under debate (50–53). These factors highlight that it is not PET but the actual evapotranspiration that drives drought. Therefore, the attribution of the observed fluctuations to climatic drivers is extremely challenging, especially if we consider the data uncertainties and the methodological limitations of casual inference techniques (54, 55). A more modest objective would be to formulate the empirical hypothesis that, since the beginning of the 21st century, warm-season droughts have been increasing concurrently with the warm-season temperatures.

The rise of compound warm-season droughts in Europe is a dynamic, developing phenomenon. It has already affected ecosystem functioning and economic growth, such as in the events of 2003 and 2018 (56, 57). A question that remains to be answered is whether this type of drought events will persist and become a common feature of European hydroclimate. The current trends in hydrological

variables derived by our analysis support that this should be anticipated to occur. In this case, compound warm-season droughts will further increase agricultural water demand, affect vegetation, and enhance the probability of firestorms (24, 58). On the other hand, the complexity of the drought phenomenon should neither be underestimated nor be oversimplified. Long-term hydrological modeling coupled with data-driven classification provides a promising framework that comes with certain limitations and assumptions. Despite the constraints, the emerging pattern presented here is a crucial first step in understanding how drought has changed in the past decades and in establishing new adaptive water management policies to mitigate the risks of future hydroclimatic hazards.

## MATERIALS AND METHODS

### Data

We use the gridded Climate Research Unit (CRU) TS (version 4.01) dataset of land surface precipitation and air temperature for the period 1901–2015 (59). We derived the monthly estimates of PET considering monthly mean temperature and the approximations for extraterrestrial solar radiation (60). The European domain was divided over three regions (fig. S1), namely, CEU, MED, and NEU. Because of discrepancies in input data, Northern Eastern Europe (Poland, Ukraine, Lithuania, Belarus, and the Baltic Sea countries), as well as some regions of MED (Southern Greece, Sicily, and central Italy) were excluded from the analysis (fig. S1, light gray areas). Another potential factor affecting the results is the varying number of stations used in the compilation of CRU dataset (59). Differences between the gridded data and gauge stations have been reported in various case studies; however, there is a consensus that, although there are biases regarding the total precipitation amount, the overall variability is generally well represented (61, 62). In addition, the influence of number of stations is higher in fine temporal scales and extreme precipitation events (63) than the monthly scale used in our analysis.

### Model

We use the grid-based, spatially explicit mHM (17, 18) to reconstruct monthly fields of grid-scaled runoff and root-zone soil moisture over the European domain since 1901 (19). The numerical approximations and conceptualizations used in the mHM are similar to well-known hydrological models such as the Hydrologiska Byråns Vattenbalansavdelning (HBV) (64) or Variable Infiltration Capacity models (65), accounting for canopy interception, snow accumulation and melting, soil moisture dynamics, infiltration and surface runoff, evapotranspiration, subsurface storage and discharge generation, deep percolation and base flow, and flood routing. A nonlinear separation scheme based on the HBV model (64) is implemented to partition incoming net rainfall into soil moisture and in/exfiltration in root-zone soil layers.

The evapotranspiration from different soil layers is modeled on the basis of available soil moisture stress and the fraction of vegetation roots in each soil layer. Different formulations of PET have been applied with no significant impact to its estimation (fig. S4). mHM considers fast- and slow-flow components for the grid-scale total runoff production. The fast-flow component is represented through a combination of a threshold-based quick interflow part and a relatively (slower) quasi-permanent interflow part with different recession constants. The slow-flow component in mHM, which reflects the groundwater contribution to runoff, is modeled as an outflow of a linear reservoir with varying recession constants

depending on the spatial heterogeneity of the underlying aquifer properties. The total runoff generated at every grid cell is routed to its neighboring downstream cell using the Muskingum routing algorithm. We used the same parameterization as in (19).

The model uses the novel multiscale parameter regionalization scheme to account for subgrid variability of landscape attributes and model parameters that allows the seamless prediction of water fluxes and states across a range of spatial scales and locations (18, 66). To date, the mHM has been previously in depth parameterized and successfully evaluated against multiple datasets (including evaporation, changes in the terrestrial water storage anomaly, and soil moisture) at multiple spatial resolutions and over a large number of river basins worldwide (66, 67). In addition, a multimodel investigation conducted recently showed a better skill of mHM in capturing the dynamics of river flow across Europe compared to more complex models like Noah-MP and PCRLOB-WB (68, 69). More details on model conceptualization and applications of mHM may be found at [www.ufz.de/mhm](http://www.ufz.de/mhm) and in (19).

### Drought events

The assessment of drought characteristics is performed across Europe at a spatial resolution of  $0.5^\circ \times 0.5^\circ$  and a monthly time step, as in (19). To determine the drought events, the standardized deficit volume was used, which measures a cumulative deviation below a preselected threshold (for fluxes, i.e., precipitation and grid-scale runoff) or considers maximum deviation below this threshold (for states, i.e., soil moisture) (16). The accumulation of the deviations below a threshold transforms the flux (runoff) into a state (volume of lacking water or its dimensionless indicator in the case of standardized data) that can be then easily compared to soil moisture deficit. The runoff/soil moisture data for each grid cell are standardized before the calculation of the deficit volume by subtracting the mean and dividing by the SD for each calendar month separately. Standardization facilitates the comparison across space and time, prevents large differences between climate types (26), and removes seasonality.

A low percentile of runoff (soil moisture) is usually considered as a threshold defining drought (19). To account for the changes in the distribution of runoff (soil moisture and precipitation) over the period 1901–2015, the 20th percentile estimated by a linear quantile regression (conditional on time) is taken as a threshold for defining drought events at each grid cell. This value is in line with the definition of drought as the deviation from (temporarily evolving) normal conditions (70) and considers adaptation to changing conditions (71, 72). We analyze time series of the maximum annual deficit volume scaled by the average annual maximum deficit volume at a grid cell. The initiation of a drought event was considered when any of the precipitation, runoff, or soil moisture standardized deficit volumes exceeded the threshold and became positive for a given grid cell. Drought termination was assumed when all three deficit volumes were zero. For the estimation of statistical significance, the nonparametric bootstrapping method was used (10,000 iterations). This approach is suitable because all the autocorrelation coefficients of all time series were close to zero. The confidence intervals (top/bottom 0.1 and 0.01 quantiles) of the average number of events over the periods that compound warm-season droughts emerged were estimated (fig. S2). These are 1995–2018 in NEU, 1989–2018 in CEU, and 1982–2018 in MED. The CoSMoS R package was used for all statistical analyses (73, 74).

### Classification

The classification framework applied is the SOM algorithm. SOM is an iterative process, which transforms the original dataset to a smaller representative set of nodes. The resulting subset is usually presented through a two-dimensional output layer (unified-distance matrix or U-Matrix), where each node corresponds to a group of members of the original dataset that share some features as determined by some distance measure (75). For readers interested in the specifics of the algorithm and its properties, we recommend the work of (21), while a review of the SOM approach in hydrology has been presented by (76).

In this study, we applied a two-layer SOM method. The first layer consisted of a  $5 \times 5 = 25$  nodes SOM. The dimensions of the SOM were determined by the variance minimization method (77). All events with duration of 3 months or more were classified over three regions (fig. S1), namely, CEU, MED, and NEU. Five variables were used for the classification: duration, month of drought event initiation, as well as first month with deficit volume in precipitation, runoff, and soil moisture during the event (fig. S5). It is important to note that for most years, six different SOM nodes describe more than 75% of the observed drought events, while more than the half are presented by the three most common SOM nodes (figs. S6 and S7). Then, the second part of classification was performed with hierarchical agglomerative clustering by Ward's method, which highlighted the three dominant groups, which correspond to approximately 90% of all nodes.

The use of a SOM was chosen as a way to tackle with the limitations of a priori classification (e.g., seasonal classes). The main downside of a priori classification is that drought events may not strictly start in the beginning of a season and, in many cases, they propagate to another season as well. It is true that our main finding is the increase of summer droughts. There are many events among these warm-season droughts, though, that start in mid or late spring and some others that end in early or mid-autumn. This is more profound in MED where the median of duration is 7 months. If seasonal classification (summer, autumn, winter, and spring) has been used instead, then the increase of warm-season droughts would be less pronounced as many of the events would be misclassified. Therefore, we encourage future studies to use SOM or other machine learning approaches for a posteriori classification.

### SUPPLEMENTARY MATERIALS

Supplementary material for this article is available at <http://advances.sciencemag.org/cgi/content/full/7/6/eabb9668/DC1>

### REFERENCES AND NOTES

1. K. Stahl, I. Kohn, V. Blauhut, J. Urquijo, L. De Stefano, V. Acácio, S. Dias, J. H. Stagge, L. M. Tallaksen, E. Kampragou, A. F. Van Loon, L. J. Barker, L. A. Melsen, C. Bifulco, D. Musolino, A. de Carli, A. Massarutto, D. Assimacopoulos, H. A. J. Van Lanen, Impacts of European drought events: insights from an international database of text-based reports. *Nat. Hazards Earth Syst. Sci.* **16**, 801–819 (2016).
2. M. Hoerling, J. Eischeid, J. Perlwitz, X. Quan, T. Zhang, P. Pegion, On the increased frequency of mediterranean drought. *J. Climate* **25**, 2146–2161 (2012).
3. J. Spinoni, G. Naumann, J. V. Vogt, Pan-european seasonal trends and recent changes of drought frequency and severity. *Global Planet. Change* **148**, 113–130 (2017).
4. L. Feyen, R. Dankers, Impact of global warming on streamflow drought in Europe. *J. Geophys. Res. Atmos.* **114**, (2009).
5. S. M. Vicente-Serrano, J.-I. Lopez-Moreno, S. Beguería, J. Lorenzo-Lacruz, A. Sanchez-Lorenzo, J. M. Garcia-Ruiz, C. Azorin-Molina, E. Morán-Tejada, J. Revuelto, R. Trigo, F. Coelho, F. Espejo, Evidence of increasing drought severity caused by temperature rise in southern Europe. *Environ. Res. Lett.* **9**, 044001 (2014).

6. L. Damberg, A. AghaKouchak, Global trends and patterns of drought from space. *Theor. Appl. Climatol.* **117**, 441–448 (2014).
7. J. Spinoni, G. Naumann, J. Vogt, P. Barbosa, European drought climatologies and trends based on a multi-indicator approach. *Global Planet. Change* **127**, 50–57 (2015).
8. A. Dai, T. Zhao, Uncertainties in historical changes and future projections of drought. Part I: Estimates of historical drought changes. *Clim. Change* **144**, 519–533 (2017).
9. A. K. Mishra, V. P. Singh, A review of drought concepts. *J. Hydrol.* **391**, 202–216 (2010).
10. Z. Hao, V. P. Singh, Drought characterization from a multivariate perspective: A review. *J. Hydrol.* **527**, 668–678 (2015).
11. K. T. Redmond, The depiction of drought: A commentary. *Bull. Am. Meteorol. Soc.* **83**, 1143–1148 (2002).
12. J. Sheffield, E. F. Wood, *Drought: Past Problems and Future Scenarios* (Routledge, 2012).
13. A. Van Loon, H. Van Lanen, A process-based typology of hydrological drought. *Hydrol. Earth Syst. Sci.* **16**, 1915–1946 (2012).
14. Y. Gao, T. Markkanen, T. Thum, M. Aurela, A. Lohila, I. Mammarella, M. Kämäräinen, S. Hagemann, T. Aalto, Assessing various drought indicators in representing summer drought in boreal forests in finland. *Hydrol. Earth Syst. Sci.* **20**, 175–191 (2016).
15. B. Heudorfer, K. Stahl, Comparison of different threshold level methods for drought propagation analysis in germany. *Hydrol. Res.* **48**, 1311–1326 (2017).
16. A. Van Loon, G. Laaha, Hydrological drought severity explained by climate and catchment characteristics. *J. Hydrol.* **526**, 3–14 (2015).
17. L. Samaniego, R. Kumar, S. Attinger, Multiscale parameter regionalization of a grid-based hydrologic model at the mesoscale. *Water Resour. Res.* **46**, W05523 (2010).
18. R. Kumar, L. Samaniego, S. Attinger, Implications of distributed hydrologic model parameterization on water fluxes at multiple scales and locations. *Water Resour. Res.* **49**, 360–379 (2013).
19. M. Hanel, O. Rakovec, Y. Markonis, P. Máca, L. Samaniego, J. Kyselý, R. Kumar, Revisiting the recent European droughts from a long-term perspective. *Sci. Rep.* **8**, 9499 (2018).
20. V. Moravec, Y. Markonis, O. Rakovec, R. Kumar, M. Hanel, A 250-year european drought inventory derived from ensemble hydrologic modeling. *Geophys. Res. Lett.* **46**, 5909–5917 (2019).
21. T. Kohonen, *Self-Organizing Maps* (Springer Series in Information Sciences, Springer, 2001), vol. 30.
22. A. AghaKouchak, L. Cheng, O. Mazdiyasi, A. Farahmand, Global warming and changes in risk of concurrent climate extremes: Insights from the 2014 california drought. *Geophys. Res. Lett.* **41**, 8847–8852 (2014).
23. F. Chiang, O. Mazdiyasi, A. AghaKouchak, Amplified warming of droughts in southern united states in observations and model simulations. *Sci. Adv.* **4**, eaat2380 (2018).
24. J. Zscheischler, S. Westra, B. J. Van Den Hurk, S. I. Seneviratne, P. J. Ward, A. Pitman, A. AghaKouchak, D. N. Bresch, M. Leonard, T. Wahl, X. Zhang, Future climate risk from compound events. *Nat. Clim. Change* **8**, 469–477 (2018).
25. J. Zscheischler, B. van den Hurk, P. J. Ward, S. Westra, in *Climate Extremes and Their Implications for Impact and Risk Assessment*, J. Sillmann, S. Sippel, S. Russo, Eds. (Elsevier, 2020), pp. 59–76.
26. A. Van Loon, E. Tjeldeman, N. Wanders, H. J. Van Lanen, A. Teuling, R. Uijlenhoet, How climate seasonality modifies drought duration and deficit. *J. Geophys. Res. Atmos.* **119**, 4640–4656 (2014).
27. T. P. Barnett, J. C. Adam, D. P. Lettenmaier, Potential impacts of a warming climate on water availability in snow-dominated regions. *Nature* **438**, 303–309 (2005).
28. S. Metsämäki, K. Böttcher, J. Pulliainen, K. Luojus, J. Cohen, M. Takala, O.-P. Mattila, G. Schwaizer, C. Derksen, S. Koponen, The accuracy of snow melt-off day derived from optical and microwave radiometer data—A study for Europe. *Remote Sens. Environ.* **211**, 1–12 (2018).
29. M. Hynčica, R. Huth, Long-term changes in precipitation phase in Europe in cold half year. *Atmos. Res.* **227**, 79–88 (2019).
30. G.-Y. Niu, Z.-L. Yang, Effects of frozen soil on snowmelt runoff and soil water storage at a continental scale. *J. Hydrometeorol.* **7**, 937–952 (2006).
31. P. Sousa, R. Trigo, P. Aizpuru, R. Nieto, L. Gimeno, R. Garcia-Herrera, Trends and extremes of drought indices throughout the 20th century in the Mediterranean. *Nat. Hazards Earth Syst. Sci.* **11**, 33–51 (2011).
32. C. Philandras, P. Nastos, J. Kapsomenakis, K. Douvis, G. Tselioudis, C. Zerefos, Long term precipitation trends and variability within the Mediterranean region. *Nat. Hazards Earth Syst. Sci.* **11**, 3235–3250 (2011).
33. C. Norrant, A. Douguédroit, Monthly and daily precipitation trends in the mediterranean (1950–2000). *Theor. Appl. Climatol.* **83**, 89–106 (2006).
34. R. Vautard, P. Yiou, F. D'andrea, N. De Noblet, N. Viovy, C. Cassou, J. Polcher, P. Ciais, M. Kageyama, Y. Fan, Summertime european heat and drought waves induced by wintertime mediterranean rainfall deficit. *Geophys. Res. Lett.* **34**, L07711 (2007).
35. Intergovernmental Panel on Climate Change, *Climate Change 2013 The Physical Science Basis: Working Group I Contribution to the Fifth Assessment Report of the Intergovernmental Panel on Climate Change* (Cambridge Univ. Press, 2014), pp. 159–254.
36. Y. Markonis, M. Hanel, P. Máca, J. Kyselý, E. Cook, Persistent multi-scale fluctuations shift european hydroclimate to its millennial boundaries. *Nat. Commun.* **9**, 1767 (2018).
37. P. Bogawski, E. Bednorz, Atmospheric conditions controlling extreme summertime evapotranspiration in Poland (Central Europe). *Nat. Hazards* **81**, 55–69 (2016).
38. D. Duethmann, G. Blöschl, Why has catchment evaporation increased in the past 40 years? A data-based study in Austria. *Hydrol. Earth Syst. Sci.* **22**, 5143–5158 (2018).
39. U. Mačček, N. Bezak, M. Šraj, Reference evapotranspiration changes in Slovenia, Europe. *Agric. For. Meteorol.* **260**, 183–192 (2018).
40. R. Právělie, A. Piticar, B. Ros, L. Sfičá, G. Bandoc, A. Tiscovschi, C. Patriche, Spatio-temporal changes of the climatic water balance in Romania as a response to precipitation and reference evapotranspiration trends during 1961–2013. *Catena* **172**, 295–312 (2019).
41. G. Laaha, T. Gauster, L. M. Tallaksen, J.-P. Vidal, K. Stahl, C. Prudhomme, B. Heudorfer, R. Vinas, M. Ionita, H. A. Van Lanen, M.-J. Adler, L. Caillouet, C. Delus, M. Fendekova, S. Gailliez, J. Hannaford, D. Kingston, A. F. Van Loon, L. Mediero, M. Osuch, R. Romanowicz, E. Sauquet, J. H. Stagge, W. K. Wong, The European 2015 drought from a hydrological perspective. *Hydrol. Earth Syst. Sci.* **21**, 3001–3024 (2017).
42. V. Hari, O. Rakovec, Y. Markonis, M. Hanel, R. Kumar, Increased future occurrences of the exceptional 2018–2019 central european drought under global warming. *Sci. Rep.* **10**, 12207 (2020).
43. B. I. Cook, T. R. Ault, J. E. Smerdon, Unprecedented 21st century drought risk in the american southwest and central plains. *Sci. Adv.* **1**, e1400082 (2015).
44. A. E. Hessel, K. J. Anchukaitis, C. Jelsema, B. Cook, O. Byambasuren, C. Leland, B. Nachin, N. Pederson, H. Tian, L. A. Hayles, Past and future drought in mongolia. *Sci. Adv.* **4**, e1701832 (2018).
45. L. Samaniego, S. Thober, R. Kumar, N. Wanders, O. Rakovec, M. Pan, M. Zink, J. Sheffield, E. Wood, A. Marx, Anthropogenic warming exacerbates European soil moisture droughts. *Nat. Clim. Change* **8**, 421–426 (2018).
46. A. G. Koutroulis, L. V. Papadimitriou, M. G. Grillakis, I. K. Tsanis, K. Wyser, R. A. Betts, Freshwater vulnerability under high end climate change. A pan-European assessment. *Sci. Total Environ.* **613–614**, 271–286 (2018).
47. M. G. Grillakis, Increase in severe and extreme soil moisture droughts for Europe under climate change. *Sci. Total Environ.* **660**, 1245–1255 (2019).
48. S. M. Vicente-Serrano, T. R. McVicar, D. G. Miralles, Y. Yang, M. Tomas-Burguera, Unraveling the influence of atmospheric evaporative demand on drought and its response to climate change. *Wiley Interdiscip. Rev. Clim. Change* **11**, e632 (2020).
49. O. Lhotka, M. Trnka, J. Kyselý, Y. Markonis, J. Balek, M. Možný, Atmospheric circulation as a factor contributing to increasing drought severity in central Europe. *J. Geophys. Res. Atmos.* **125**, e2019JD032269 (2020).
50. S. Fatchi, S. Leuzinger, A. Paschalis, J. A. Langley, A. D. Barraclough, M. J. Hovenden, Partitioning direct and indirect effects reveals the response of water-limited ecosystems to elevated CO<sub>2</sub>. *Proc. Natl. Acad. Sci. U.S.A.* **113**, 12757–12762 (2016).
51. T. Mastrotheodoros, C. Pappas, P. Molnar, P. Burlando, T. F. Keenan, P. Gentine, C. M. Gough, S. Fatchi, Linking plant functional trait plasticity and the large increase in forest water use efficiency. *J. Geophys. Res. Biogeo.* **122**, 2393–2408 (2017).
52. M. Berdugo, M. Delgado-Baquerizo, S. Soliveres, R. Hernández-Clemente, Y. Zhao, J. J. Gaitán, N. Gross, H. Saiz, V. Maire, A. Lehman, M. C. Rillig, R. V. Solé, F. T. Maestre, Global ecosystem thresholds driven by aridity. *Science* **367**, 787–790 (2020).
53. T. F. Keenan, X. Luo, Y. Zhang, S. Zhou, Ecosystem aridity and atmospheric CO<sub>2</sub>. *Science* **368**, 251–252 (2020).
54. J. Runge, S. Bathiany, E. Bollt, G. Camps-Valls, D. Coumou, E. Deyle, C. Glimour, M. Kretschmer, M. D. Mahecha, J. Muñoz-Mari, E. H. van Nes, J. Peters, R. Quax, M. Reichstein, M. Scheffer, B. Schölkopf, P. Spirtes, G. Sugihara, J. Sun, K. Zhang, J. Zscheischler, Inferring causation from time series in earth system sciences. *Nat. Commun.* **10**, 2553 (2019).
55. M. Ombadi, P. Nguyen, S. Sorooshian, K.-I. Hsu, Evaluation of methods for causal discovery in hydrometeorological systems. *Water Resour. Res.* **56**, e2020WR027251 (2020).
56. P. Ciais, M. Reichstein, N. Viovy, A. Granier, J. Ogée, V. Allard, M. Aubinet, N. Buchmann, C. Bernhofer, A. Carrara, F. Chevallier, N. De Noblet, A. D. Friend, P. Friedlingstein, T. Grünwald, B. Heinesch, P. Kerönen, A. Knohl, G. Krinner, D. Loustau, G. Manca, G. Matteucci, F. Miglietta, J. M. Ourcival, D. Papale, K. Pilegaard, S. Rambal, G. Seufert, J. F. Soussana, M. J. Sanz, E. D. Schulze, T. Vesala, R. Valentini, Europe-wide reduction in primary productivity caused by the heat and drought in 2003. *Nature* **437**, 529–533 (2005).
57. T. Mastrotheodoros, C. Pappas, P. Molnar, P. Burlando, G. Manoli, J. Parajka, R. Rigon, B. Szeles, M. Bottazzi, P. Hadjidoukas, S. Fatchi, More green and less blue water in the alps during warmer summers. *Nat. Clim. Change* **10**, 155–161 (2020).
58. A. F. Van Loon, T. Gleeson, J. Clark, A. I. Van Dijk, K. Stahl, J. Hannaford, G. Di Baldassarre, A. J. Teuling, L. M. Tallaksen, R. Uijlenhoet, D. M. Hannah, J. Sheffield, M. Svoboda, B. Verbeiren, T. Wagener, S. Rangelcroft, N. Wanders, H. A. J. Van Lanen, Drought in the anthropocene. *Nat. Geosci.* **9**, 89–91 (2016).

59. I. Harris, P. Jones, T. Osborn, D. Lister, Updated high-resolution grids of monthly climatic observations – the CRU TS3.10 Dataset. *Int. J. Climatol.* **34**, 623–642 (2014).
60. L. Oudin, F. Hervieu, C. Michel, C. Perrin, V. Andréassian, F. Anctil, C. Loumagne, Which potential evapotranspiration input for a lumped rainfall–runoff model?: Part 2—Towards a simple and efficient potential evapotranspiration model for rainfall–runoff modelling. *J. Hydrol.* **303**, 290–306 (2005).
61. H. Shi, T. Li, J. Wei, Evaluation of the gridded cru ts precipitation dataset with the point raingauge records over the three-river headwaters region. *J. Hydrol.* **548**, 322–332 (2017).
62. S. Herrera, S. Kotlarski, P. M. Soares, R. M. Cardoso, A. Jaczewski, J. M. Gutiérrez, D. Maraun, Uncertainty in gridded precipitation products: Influence of station density, interpolation method and grid resolution. *Int. J. Climatol.* **39**, 3717–3729 (2019).
63. K. Schroerer, G. Kirchengast, S. O. Strong dependence of extreme convective precipitation intensities on gauge network density. *Geophys. Res. Lett.* **45**, 8253–8263 (2018).
64. G. Lindström, B. Johansson, M. Persson, M. Gardelin, S. Bergström, Development and test of the distributed hbv-96 hydrological model. *J. Hydrol.* **201**, 272–288 (1997).
65. X. Liang, E. F. Wood, D. P. Lettenmaier, Surface soil moisture parameterization of the vic-2l model: Evaluation and modification. *Global Planet. Change* **13**, 195–206 (1996).
66. O. Rakovec, R. Kumar, J. Mai, M. Cuntz, S. Thober, M. Zink, S. Attinger, D. Schäfer, M. Schrön, L. Samaniego, Multiscale and multivariate evaluation of water fluxes and states over European river basins. *J. Hydrometeorol.* **19**, 287–307 (2016).
67. R. Kumar, B. Livneh, L. Samaniego, Toward computationally efficient large-scale hydrologic predictions with a multiscale regionalization scheme. *Water Resour. Res.* **49**, 5700–5714 (2013).
68. S. Thober, R. Kumar, N. Wanders, A. Marx, M. Pan, O. Rakovec, L. Samaniego, J. Sheffield, E. F. Wood, M. Zink, Multi-model ensemble projections of european river floods and high flows at 1.5, 2, and 3 degrees global warming. *Environ. Res. Lett.* **13**, 014003 (2018).
69. A. Marx, R. Kumar, S. Thober, O. Rakovec, N. Wanders, M. Zink, E. F. Wood, M. Pan, J. Sheffield, L. Samaniego, Climate change alters low flows in europe under global warming of 1.5, 2, and 3 c. *Hydrol. Earth Syst. Sci.* **22**, 1017–1032 (2018).
70. L. M. Tallaksen, H. A. Van Lanen, *Hydrological Drought: Processes and Estimation Methods for Streamflow and Groundwater* (Elsevier, 2004), vol. 48.
71. J.-P. Vidal, E. Martin, N. Kitova, J. Najac, J.-M. Soubeyroux, Evolution of spatio-temporal drought characteristics: validation, projections and effect of adaptation scenarios. *Hydrol. Earth Syst. Sci.* **16**, 2935–2955 (2012).
72. N. Wanders, Y. Wada, H. Van Lanen, Global hydrological droughts in the 21st century under a changing hydrological regime. *Earth Syst. Dynam.* **6**, 1–15 (2015).
73. S. M. Papalexiou, Unified theory for stochastic modelling of hydroclimatic processes: Preserving marginal distributions, correlation structures, and intermittency. *Adv. Water Resour.* **115**, 234–252 (2018).
74. S. M. Papalexiou, Y. Markonis, F. Lombardo, A. AghaKouchak, E. Foufoula-Georgiou, Precise temporal disaggregation preserving marginals and correlations (dipmac) for stationary and nonstationary processes. *Water Resour. Res.* **54**, 7435–7458 (2018).
75. A. Ultsch, H. P. Siemon, Kohonen's self organizing feature maps for exploratory data analysis, in *Proceedings of the International Neural Network Conference (INNC-90), Paris, France, July 9–13, 1990*. Dordrecht, Netherlands, B. Widrow, B. Angeniol, Eds. (Kluwer Academic Press, 1990), vol. 1, pp. 305–308.
76. A. M. Kalteh, P. Hjorth, R. Berndtsson, Review of the self-organizing map (som) approach in water resources: Analysis, modelling and application. *Environ. Model. Software* **23**, 835–845 (2008).
77. Y. Markonis, F. Strnad, Representation of European hydroclimatic patterns with self-organizing maps. *The Holocene* **30**, 1155–1162 (2020).

**Acknowledgments:** We would like to thank C. Miao and Z. Hao for valuable feedback in earlier versions of the analysis and the four anonymous reviewers for constructive comments. Y.M. would also like to thank C. Pappas, V. Moravec, and J. Schurman for fruitful conversations on the topic, as well as V. Pandou for help in polishing the figures.

**Funding:** This work was partially funded by a bilateral project XEROS (eXtreme EuRopean drOughtS: multimodel synthesis of past, present, and future events), by the Czech Science Foundation (grant no. 19-24089 J), and by the Deutsche Forschungsgemeinschaft (grant RA 3235/1-1). This study was also partially funded by the Internal Grant Agency of the Faculty of Environmental Sciences of Czech University of Life Sciences (grant no. 42200/1312/3171). **Author contributions:** Y.M. conceived the original idea, which was further developed by M.H. and P.M. Hydrologic modeling was performed by O.R. and R.K. Y.M. designed the empirical experiments and conducted the statistical analyses. All authors contributed to the interpretation and discussion of the results. The manuscript was written by Y.M., R.K., and A.A. **Competing interests:** The authors declare that they have no competing interests. **Data and materials availability:** All data needed to evaluate the conclusions in the paper are present in the paper and/or the Supplementary Materials. Additional data related to this paper may be requested from the authors.

Submitted 30 March 2020

Accepted 17 December 2020

Published 3 February 2021

10.1126/sciadv.abb9668

**Citation:** Y. Markonis, R. Kumar, M. Hanel, O. Rakovec, P. Máca, A. AghaKouchak, The rise of compound warm-season droughts in Europe. *Sci. Adv.* **7**, eabb9668 (2021).

## The rise of compound warm-season droughts in Europe

Yannis MarkonisRohini KumarMartin HanelOldrich RakovecPetr MácaAmir AghaKouchak

*Sci. Adv.*, 7 (6), eabb9668.

### View the article online

<https://www.science.org/doi/10.1126/sciadv.abb9668>

### Permissions

<https://www.science.org/help/reprints-and-permissions>

Use of think article is subject to the [Terms of service](#)

---

*Science Advances* (ISSN 2375-2548) is published by the American Association for the Advancement of Science. 1200 New York Avenue NW, Washington, DC 20005. The title *Science Advances* is a registered trademark of AAAS.

Copyright © 2021 The Authors, some rights reserved; exclusive licensee American Association for the Advancement of Science. No claim to original U.S. Government Works. Distributed under a Creative Commons Attribution NonCommercial License 4.0 (CC BY-NC).